JOURNAL OF SOLID STATE CHEMISTRY **122,** 239–244 (1996)
ARTICLE NO. 0107

Crystal and Electronic Structure of a Quaternary Layered Compound from the K–In–Ge–Sb System: $K_9In_9GeSb_{22}$

Julie L. Shreeve-Keyer and Robert C. Haushalter

NEC Research Institute, 4 Independence Way, Princeton, New Jersey 08540

and

Dong-Kyun Seo and Myung-Hwan Whangbo

Department of Chemistry, North Carolina State University, Raleigh, North Carolina 27695

Received July 25, 1995; in revised form December 15, 1995; accepted December 19, 1995

The quaternary Zintl phase material, $K_9In_9GeSb_{22}$ (1), has been prepared at 650°C and its structure determined by single crystal X-ray diffraction: triclinic, space group $P\bar{1}$ with a = 11.62 (1) Å, b = 13.04 (3) Å, c = 11.27 (2) Å, α = 113.5 (2)°, β = 91.7 (1)°, γ = 112.3 (1)°, V = 1415 (4) Å^3, and D_{calcd} = 4.851 g/cm^3 for Z = 2 and $R(R_w)$ = 7.9% (8.8%). Antimonide 1 contains layers comprised of indium, germanium, and arsenic separated by K^+ cations. The In–Ge–Sb layers in 1 contain $In_{(2-x)}Ge_xSb_6$ ($x \cong 1$) dimers with In(Ge)–In(Ge) bonds, $InSb_4$ tetrahedra, and Sb_3 trimers, as well as infinite chains with Sb–Sb bonds. There is an unusual metal–metal bonded site in 1, that contains contains a solid solution of 1:1 In and Ge, with an In(Ge)–In(Ge) separation of 2.659 (1) Å. The nature of this experimentally determined solid solution at the M–M bonded site, and its effects on the electronic structure of $K_9In_9GeSb_{22}$, was investigated via tight binding calculations. © 1996 Academic Press, Inc.

INTRODUCTION

Both the structures and properties of the Zintl phase materials are unique among solid state inorganic compounds. The Zintl phase compounds are often considered as possessing properties intermediate between those of ionic salts and metals or intermetallic phases. Typically, the reaction between an alkali or alkaline earth metal and a heavier post-transition element results in electron transfer from the more electropositive elements to the post-transition elements. This sometimes results in the formation of isolated covalently bonded polyatomic anionic units, commonly referred to as Zintl anions. The elements that comprise these materials, for example an alkaline earth metal and a heavy main group element, will often transfer electrons in order to achieve an octet in the valence electron shell of the elements within the anion combined with alkaline earth cations. Because the resulting anions are often electron precise and diamagnetic, these materials would normally be expected to exhibit semiconducting behavior.

In recent years, there has been a renewed interest in Zintl phase materials, with reports of the synthesis of new materials by Schäfer and co-workers (1), von Schnering and co-workers (2), Corbett and co-workers (3), Cordier and co-workers (4), Asbrand and Eisenmann (5), Belin and co-workers (6), and others (7). Several Group I–In–Sb materials and one K–In–Ge Zintl phase have appeared in the literature including $K_2NaInSb_2$ (2a), Na_3InSb_2 (8), $K_{10}In_5Sb_9$ (4e), $K_4In_4Sb_6$ (6), $M_2In_2Sb_3$ (M = K(9), Na(10)), Cs_6InSb_3 (11), and $K_8In_6Ge_{40}$ (12) but structurally characterized Group I–Ge–Sb or Group I–In–Ge–Sb materials appear to be rare or nonexistent. We report here the preparation and structural characterization of a new quarternary I–III–IV–V Zintl phase material, $K_9In_9GeSb_{22}$ (**1**), which has a complicated layered structure composed of In–Ge–Sb layers alternating with interlayer K^+ ions. The In–Ge–Sb layers in **1** contain novel $In_{(2-x)}Ge_xSb_6$ ($x \cong 1$) dimers with In(Ge)–In(Ge) bonds, $InSb_4$ tetrahedra, and Sb_3 trimers, as well as an infinite, puckered chain of Sb atoms. The substitution of 50% germanium into a single one of the many indium sites results in an electron precise material. The implication of the Ge at this site was investigated by extended Hückel tight binding calculations which confirmed the closed shell nature of the polyanionic layer.

EXPERIMENTAL DETAILS

Preparation of $K_9In_9GeSb_{22}$ (**1**). Compound **1** is extremely air- and moisture-sensitive, and all manipulations were performed using standard inert atmosphere techniques. Single crystals of X-ray quality of compound **1** were

0022-4596/96 $18.00

TABLE 1
Experimental Data for the X-Ray Diffraction Study of $K_9In_9GeSb_{22}$

Empirical formula	$K_{4.5}In_{4.5}Ge_{0.5}Sb_{11}$
FW (g/mol)	2068.18
Temp. (K)	293
Crystal color, habit	Dark silver, plate
Crystal dimensions (mm)	Approx. 0.05 × 0.20 × 0.20
Crystal system	Triclinic
Space group	$P\bar{1}$
a (Å)	11.62 (1)
b (Å)	13.04 (3)
c (Å)	11.27 (2)
α (deg)	113.5 (2)
β (deg)	91.7 (1)
γ (deg)	112.3 (1)
Volume (Å^3)	1415 (4)
Z	2
D_{calcd} (g/cm^3)	4.851
Diffractometer	Rigaku AFC7R
Scan type	ω-2θ
Scan rate	16.0°/min (in ω)
2θ(max) (deg)	50.1
μ(Mo$K\alpha$), cm^{-1}	149.12
Reflections collected	5087
Unique reflections	4375
Observed reflections ($I > 3.00\ \sigma(I)$)	2784
No. of Variables	187
R, R_w	7.9%, 8.8%
Goodness of fit	4.82
Maximum peak in final diff. map (e/Å^3)	3.49
Minimum peak in final diff. map (e/Å^3)	−3.88

prepared by heating a mixture of K_3Sb_7, Sb, In, and Ge in a 5 : 7 : 12 : 18 mole ratio, in an evacuated, sealed quartz tube. The sample was heated to 650°C over 12 h, where the temperature was held for an additional 2 h. The sample was cooled at a linear rate to 500°C over 48 h, and then cooled to ambient temperature over 12 h. Air-sensitive crystals of **1**, as well as crystals of Ge metal, and small amounts of InSb and Sb were present in the crushed regulus according to powder X-ray diffraction measurements (Scintag XDS 2000). Energy dispersive spectroscopy (EDS) analysis (Princeton Gamma Tech EDS detector, Hitachi S-2700 SEM) of **1** on both the surface and the interior of the crystals showed them to contain K, In, Ge, and Sb in approximately a 12 : 9 : 1 : 22 ratio.

Crystallography. Data was collected on a dark silver plate, of approximate dimensions 0.05 × 0.20 × 0.20 mm^3, mounted in a helium filled glass capillary. Experimental details are listed in Table 1 and the final fractional coordinates for **1** are found in Table 2.

RESULTS AND DISCUSSION

During our investigations of new quaternary Zintl phase materials (13), we prepared single crystals of $K_9In_9GeSb_{22}$ (**1**) from the thermal treatment of K_3Sb_7, Sb, In, and Ge, at 650°C in a sealed quartz tube. In addition to antimonide **1**, the melt also contained Ge metal and small amounts of InSb and Sb, but no attempt was made to optimize the yield or phase purity.

The initial solution of the X-ray data revealed K^+ cations and layers composed only of indium and anitmony which refined to $R \cong 8\%$. However, if one assigns the typical oxidation states of +1 to potassium, +3 to indium, −3 to the isolated antimony, and $-(3 - n)$ to the antimony atoms coordinated to n other antimony atoms, the formula $K_9In_{10}Sb_{22}$ is not electron precise. Inspection of the isotropic thermal parameters at this point revealed that In(1) had a value of $B_{iso} = 3.10\ (8)$ Å^2 which was roughly twice as large as the isotropic thermal parameters of most of the other layer atoms in the structure. A model which contained Ge and In at the In(1) site was developed and proved reasonable for several reasons. First, the 2.659 (1) Å In(Ge)–In(Ge) bond distance in **1** is much shorter than the 2.923 (1) Å In–In distance in the In_2Sb_6 dimer found in $K_5In_{10}Sb_9$ (4e) or the 3.25 and 3.38 Å In–In distances found in indium metal (14). The 2.659 (1) Å distance is also somewhat shorter than the In–In bonds in the range from 2.770 (4) to 2.790 (4) Å in In_4Te_3 (15) and 2.858 (3) Å in $Na_7In_{11.76}$ (16). The 2.659 (1) Å distance is however significantly longer than the Ge–Ge bond contact of 2.43

TABLE 2
Fractional Atomic Coordinates and Equivalent Isotropic Thermal Parameters (Å^2) for $K_9In_9GeSb_{22}$

Atom	x	y	z	B_{eq}[a]	Occupancy
Sb(1)	0.5155(3)	0.0662(2)	0.1384(3)	1.88(6)	1.000
Sb(2)	0.4898(3)	0.2748(2)	0.1341(3)	1.63(6)	1.000
Sb(3)	0.5187(3)	0.2339(2)	0.8739(3)	1.75(6)	1.000
Sb(4)	0.5812(3)	0.4803(2)	0.9163(3)	1.87(6)	1.000
Sb(5)	0.1959(3)	0.3710(2)	0.8783(3)	1.50(5)	1.000
Sb(6)	0.2469(3)	0.0783(2)	0.4831(3)	1.35(5)	1.000
Sb(7)	−0.0833(3)	0.1749(2)	0.6160(3)	1.46(5)	1.000
Sb(8)	−0.0936(3)	0.0151(2)	0.1736(3)	1.43(5)	1.000
Sb(9)	0.2338(3)	0.4079(2)	0.4728(3)	1.49(5)	1.000
Sb(10)	0.2368(3)	0.7389(2)	0.4821(3)	1.59(5)	1.000
Sb(11)	−0.0842(3)	0.3635(2)	0.1733(3)	1.65(6)	1.000
In(1)	0.0752(3)	0.4971(3)	0.4132(4)	1.91(5)	0.500
In(2)	0.2594(3)	0.1670(2)	0.7593(3)	1.36(6)	1.000
In(3)	0.0700(3)	0.1633(2)	0.4261(3)	1.40(6)	1.000
In(4)	0.2572(3)	0.5284(2)	0.7493(3)	1.36(5)	1.000
In(5)	0.7820(3)	0.1713(2)	0.2452(3)	1.48(6)	1.000
Ge(1)	0.0752(3)	0.4971(3)	0.4132(4)	1.91(5)	0.500
K(1)	0.1717(9)	0.2609(8)	0.127(1)	2.2(2)	1.000
K(2)	0.854(1)	0.3893(10)	0.871(1)	3.6(3)	1.000
K(3)	0.8128(10)	0.059(1)	0.877(1)	3.6(3)	1.000
K(4)	0.506(1)	0.358(1)	0.547(1)	4.5(3)	1.000
K(5)	0.5000	0.0000	0.5000	7.8(6)	0.500

[a] $B_{eq} = 8/3\pi^2(U_{11}(aa^*)^2 + U_{22}(bb^*)^2 + U_{33}(cc^*)^2 + 2U_{12}aa^*bb^*\cos\gamma + 2U_{13}aa^*cc^*\cos\beta + 2U_{23}bb^*cc^*\cos\alpha)$.

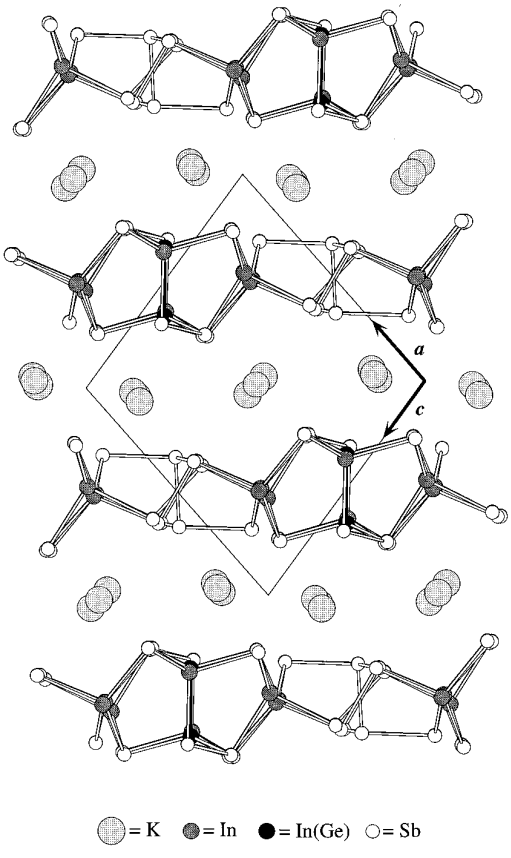

FIG. 1. View of $K_9In_9GeSb_{22}$ (**1**) showing unit cell, down *b* axis.

(1) Å observed in Ge_2As_6 dimers in $K_8In_8Ge_5As_{14}(As_3)$ (13). The In(Ge)–In(Ge) bond length in **1** falls approximately midway between these distances. Also, the average In(Ge)–Sb bond distance of 2.71 (2) Å is shorter than the 2.84(2) Å average In–Sb distance for the rest of the atoms (Table 3). Second, EDS analysis of the both the surface and interior of the crushed data crystal showed the presence of germanium and indium in approximately a 1:9 ratio. Third, the refinement of the X-ray data was consistent with the partial occupancy of Ge in the In(1) site. Originally, In(1) was refined as 100% In, which resulted in a rather high thermal parameter of $B_{eq} = 3.10$ (8) for this atom. The thermal parameters for several of the atoms, especially In(1) which was reduced to a value ($B_{eq} = 1.91$ (5) Å^2) much closer to the other In atoms in the structure, became much more reasonable (Table 4) upon refining the site as 50% Ge and 50% In. The model which contained partial Ge occupancy also resulted in better values for R and (R_w), which were lowered slightly from $R(R_w)$ = 8.2%(9.1%) for the model with 100% In occupancy at In(1) to $R(R_w)$ = 7.9%(8.8%) (Table 1) for the model with the partial occupancy. The extreme shortening of the In(Ge)–In(Ge) bond, coupled with the EDS analysis and the refinement of the X-ray data, is consistent with the 50% partial occupancy of Ge in the In(1) site.

Further support of this model is provided by investigating the electronic structures of $K_9In_{10}Sb_{22}$ and $K_9In_9GeSb_{22}$ via extended Hückel tight binding calculations (17) carried out for the $In_{10}Sb_{22}^{9-}$ and $In_9GeSb_{22}^{9-}$ lattices, respectively. $K_9In_{10}Sb_{22}$ is electron-imprecise, so its electronic band structure has a half-filled narrow band (Fig. 2a), which lies well above the top of the completely filled bands lying below (by about 2 eV). Analysis of the orbital compositions of the density of states (DOS) reveals that the half-filled narrow band is largely associated with the sigma bonding level of the In(1)–In(1) pair. An ordered form of the electron-precise formula $K_9In_9GeSb_{22}$ results when one of the two In(1) atom sites of $K_9In_{10}Sb_{22}$ is replaced with a Ge atom. In the electronic structure calculated for this form of $K_9In_9GeSb_{22}$, there is no partially filled band (Fig. 2b). Analysis of the orbital compositions of the DOS shows that the completely-filled narrow band lying at the top of the valence bands is largely associated with the sigma bonding level of the In(1)–Ge pair. This band lies about 1.7 eV below the half-filled narrow band found for $K_9In_{10}Sb_{22}$. This means that, given the bond distance of 2.695 (1) Å for the In(1)–Ge and In(1)–In(1) pairs, a stronger overlap occurs between the sp^3 orbitals of the In(1) and Ge atoms than between those of the two In(1) atoms. Consequently, from the viewpoint of electronic energy as well, the electron-precise formula $K_9In_9GeSb_{22}$ in which half occupancy of Ge occurs at the In(1) sites is preferred to the electron-imprecise formula $K_9In_{10}Sb_{22}$.

A polyhedral representation of a single layer of compound **1** is shown in Fig. 3. Each layer, which lies in a plane parallel to (1 0 $\bar{1}$), contains $In_{(2-x)}Ge_xSb_6$ ($x \cong 1$) dimers, $InSb_4$ tetrahedra, Sb_3 units, and infinite Sb chains. The structure of an individual layer can be described by examining the rows that run parallel to the *b* axis formed by the indium-centered $InSb_4$ tetrahedra and antimony chains. There is a slab of three rows of In(Ge)–Sb and In–Sb polyhedra, which is connected to the next set of three rows by a puckered Sb chain containing Sb–Sb bonds. The center row of the polyhedra contains $InSb_4$ tetrahedra and $In_{(2-x)}Ge_xSb_6$ dimers. These are arranged in a regular fashion, such that a dimer, whose In(Ge)–In(Ge) bond is roughly perpendicular to the plane of the layer, is connected through one corner on either side to an $InSb_4$ tetrahedron. The tetrahedra are related by an inversion center located at the midpoint of the In(Ge)–In(Ge) bond in the dimer.

The vertices of the two indium centered tetrahedra on either side of the $In_{(2-x)}Ge_xSb_6$ dimer, within the same row, are facing in opposite directions, or each to a different side of the layer, related to one another by the inversion center located at the midpoint of the In(Ge)–In(Ge) bond in the dimer. One Sb atom on the vertex of each of the $InSb_4$

TABLE 3
Selected Atomic Distances (Å) for $K_9In_9GeSb_{22}$

Atom	Atom	Distance	Atom	Atom	Distance	Atom	Atom	Distance
Sb(1)	Sb(1)	2.831(6)	Sb(5)	In(2)	2.851(4)	Sb(8)	In(3)	2.821(4)
Sb(1)	Sb(2)	2.865(4)	Sb(5)	In(4)	2.858(4)	Sb(9)	In(3)	2.841(4)
Sb(1)	In(1)	2.856(5)	Sb(6)	Sb(7)	2.817(4)	Sb(9)	In(4)	2.825(4)
Sb(2)	Sb(3)	2.819(5)	Sb(6)	In(2)	2.833(4)	Sb(9)	In(1)	2.715(4)
Sb(2)	In(4)	2.883(4)	Sb(6)	In(3)	2.844(5)	Sb(10)	In(5)	2.870(4)
Sb(3)	Sb(4)	2.839(4)	Sb(7)	Sb(10)	2.838(5)	Sb(10)	In(1)	2.746(3)
Sb(3)	In(2)	2.896(5)	Sb(7)	In(3)	2.820(5)	Sb(11)	In(5)	2.845(4)
Sb(4)	Sb(4)	2.750(7)	Sb(8)	In(5)	2.807(5)	Sb(11)	In(4)	2.840(5)
Sb(4)	Sb(5)	2.843(4)	Sb(8)	In(2)	2.823(4)	Sb(11)	In(1)	2.698(3)
In(1)/Ge(1)	In(1)/Ge(1)	2.659(1)						
K(1)	Sb(2)	3.63(1)	K(2)	Sb(5)	3.53(1)	K(3)	Sb(8)	3.80(1)
K(1)	Sb(4)	3.73(1)	K(2)	Sb(7)	3.45(1)	K(3)	Sb(11)	3.73(1)
K(1)	Sb(5)	3.60(1)	K(2)	Sb(10)	3.59(1)	K(4)	Sb(4)	3.75(2)
K(1)	Sb(8)	3.59(1)	K(2)	Sb(11)	3.63(1)	K(4)	Sb(6)	3.51(1)
K(1)	Sb(8)	3.74(1)	K(2)	Sb(11)	3.56(1)	K(4)	Sb(9)	3.48(1)
K(1)	Sb(9)	3.49(1)	K(3)	Sb(1)	3.50(1)	K(4)	Sb(9)	3.60(1)
K(1)	Sb(11)	3.67(1)	K(3)	Sb(6)	3.65(1)	K(4)	Sb(10)	3.64(1)
K(2)	Sb(3)	3.65(1)	K(3)	Sb(7)	3.85(1)	K(5)	Sb(6)	3.482(4)
K(2)	Sb(4)	3.76(1)	K(3)	Sb(8)	3.73(1)	K(5)	Sb(10)	3.536(3)

tetrahedra in the center row is not shared with other polyhedra, and as a result forms bonds with two other Sb atoms from $InSb_4$ in the neighboring rows to form an Sb_3 unit with two Sb–Sb bonds. One can think of the formation of the Sb_3 units in the following way: when an $In_{(2-x)}Ge_x$ Sb_6 dimer is replaced by an $InSb_4$ tetrahedron, the Sb atoms link via Sb–Sb bonds to satisfy their coordination change resulting from the ''missing'' indium atom to form an Sb_3 unit with two Sb–Sb bonds. Similarly, the formation of As_3 units has been observed in $K_8In_8Ge_5As_{14}(As_3)$ (13). The resulting Sb_3 units contain 2.817 (4) and 2.838 (5) Å Sb–Sb distances and an Sb–Sb–Sb angle of 101.4 (1)°. The $InSb_4$–$In_{(2-x)}Ge_xSb_6$–$InSb_4$ unit is repeated along the row.

TABLE 4
Comparison of Equivalent Isotropic Thermal Parameters (Å²) and Refinement Values for $K_9In_{10}Sb_{22}$ and $K_9In_9GeSb_{22}$

	$K_9In_{10}Sb_{22}$		$K_9In_9GeSb_{22}$	
Atom	B_{eq}	Occupancy	B_{eq}	Occupancy
In(1)	3.1(1)	1.000	1.91(5)	0.500
In(2)	1.31(9)	1.000	1.36(6)	1.000
In(3)	1.28(8)	1.000	1.40(6)	1.000
In(4)	1.31(8)	1.000	1.36(5)	1.000
In(5)	1.36(8)	1.000	1.48(6)	1.000
Ge(1)	—	0.000	1.91(5)	0.500
R (R_w)	8.0% (9.1%)		7.9% (8.8%)	
GOF	5.04		4.82	

Along the outer edges of the slab are rows of $InSb_4$ tetrahedra which form corner-sharing interactions with one another as well as to the center row of polyhedra through Sb atoms.

The infinite one-dimensional antimony chain which links the three-polyhedra-thick slab is shown in Fig. 4. Infinite Sb–Sb bonded chains have not been observed in other Group I–In–Sb structures (2a, 4e, 6, 8–10) or Group I–Ge–Sb structures. The Sb–Sb bond distances along the chain range from 2.750 (7) to 2.865 (4) Å. The eight Sb–Sb contacts within the centrosymmetric translational repeat of the Sb–Sb bonded chain are also depicted in Fig. 4. There is a $\bar{1}$ site which lies on the midpoint of the bond connecting the two central Sb atoms, Sb(4), of the translational repeat. These two Sb(4) atoms are each bonded only to Sb atoms and do not contact any In centers as do the remaining atoms in the chain, Sb atoms Sb(1), Sb(2), and Sb(3). Compound **1** is significantly more antimony-rich than $K_{10}In_5Sb_9$ (4e) and $K_4In_4Sb_6$ (6, 9), which could account for the formation of the Sb chain and high degree of Sb–Sb bonding in this structure.

There are five crystallographically independent potassium cations in compound **1**. The coordination environment for each potassium atom is shown in Fig. 5 while the potassium antimony distances are given in Table 3. Potassium atoms 1 and 2 are both formally seven-coordinated. Potassium atom 3 is coordinated to six antimony atoms. The geometry around potassium 4 is that of a slightly distorted square pyramid. Potassium atom 5 is coordinated to only four antimony atoms in nearly a square planar arrangement.

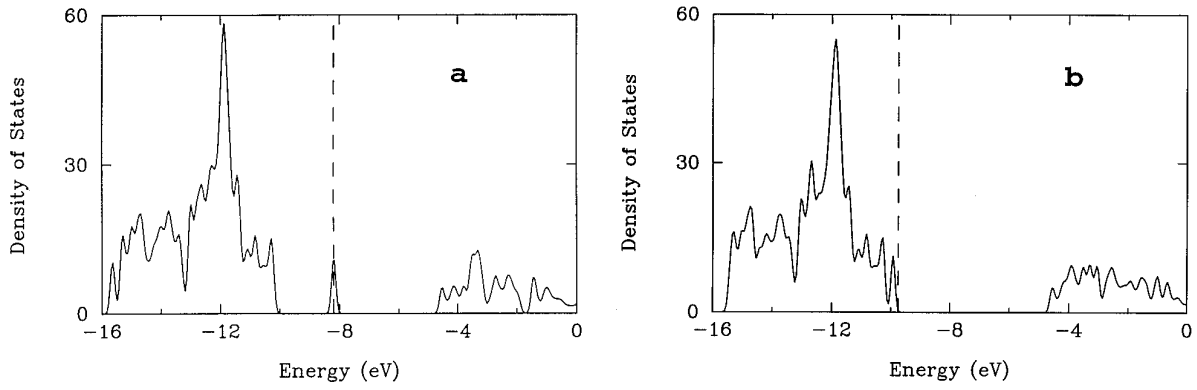

FIG. 2. Density of states (DOS) calculated for (a) the $In_{10}Sb_{22}^{9-}$ lattice of $K_9In_{10}Sb_{22}$ and (b) the $In_9GeSb_{22}^{9-}$ lattice of the ordered form of $K_9In_9GeSb_{22}$ (see the text). The vertical broken line refers to the highest occupied level, and the DOS values are given in electrons per formula unit.

Compound **1** is related to $K_{10}In_5Sb_9$ (4e) and $K_4In_4Sb_6$ (6) ($K_2In_2Sb_3$ (9) and $K_4In_4Sb_6$ (6) have the same structure) in that all of these compounds have layers which contain indium and antimony, separated by K^+ cations. However, the structures which are formed in these three systems are quite different. The compound $K_{10}In_5Sb_9$ (4e) contains layers formed from $InSb_4$ tetrahedra and In_2Sb_6 dimers connected by common edges and corners, as well chains of $InSb_4$ tetrahedra connected by common edges and additional Sb atoms. The $InSb_4$ chains and the potassium cations lie between the layers. The layers in $K_{10}In_5Sb_9$ are more open than in compound **1**, and are formed by units which are comprised of two edge sharing In_2Sb_6 dimers and one $InSb_4$ tetrahedra. Unlike in compound **1**, the In–In bonds in $K_9In_5Sb_9$ are roughly parallel to the plane of the layer. The structure of **1** is more similar to $K_4In_4Sb_6$ (6) in that both consist of layers of In–Sb separated by K^+ ions, and no In–Sb chains. The layers in $K_4In_4Sb_6$ are formed by $InSb_4$ tetrahedra which are connected by common corners and edges, and contain Sb_2 groups. The 2.866 (1) Å Sb–Sb distance in $K_4In_4Sb_6$ is comparable to the range of Sb–Sb distances observed in **1**.

Compound **1** is, to the best of our knowledge, the first compound obtained from the K–In–Ge–Sb system. To date, only Group I–In–Sb materials and one K–In–Ge compound are known. The K–In–Sb systems which have been previously structurally characterized also contain In–Sb layers separated by potassium cations, suggesting this may be a common motif for this type of structure. It is somewhat surprising that it is possible to make such complicated structures at such relatively high temperatures and that a quaternary material such as **1** can exist without disproportionation into binary phases. Further work is required to delineate the thermal and phase stabilities of these quaternary materials but we will shortly report on

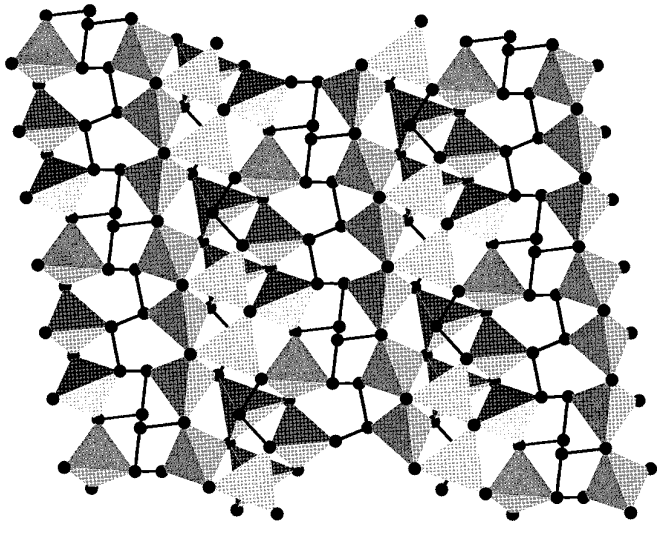

FIG. 3. A polyhedral representation of a single layer in **1**.

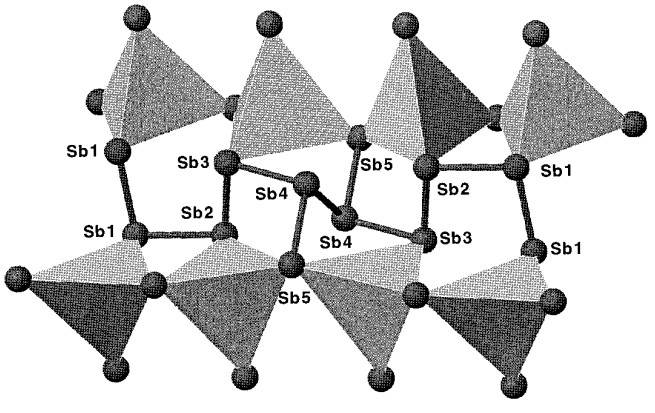

FIG. 4. View of antimony chain in **1**. Some important bond distances: Sb(1) − Sb(1), 2.831 (6) Å; Sb(1) − Sb(2), 2.865 (4) Å; Sb(2) − Sb(3), 2.819 (5) Å; Sb(3) − Sb(4), 2.834 (4) Å; Sb(4) − Sb(4), 2.750 (7) Å; Sb(4) − Sb(5), 2.843 (4) Å.

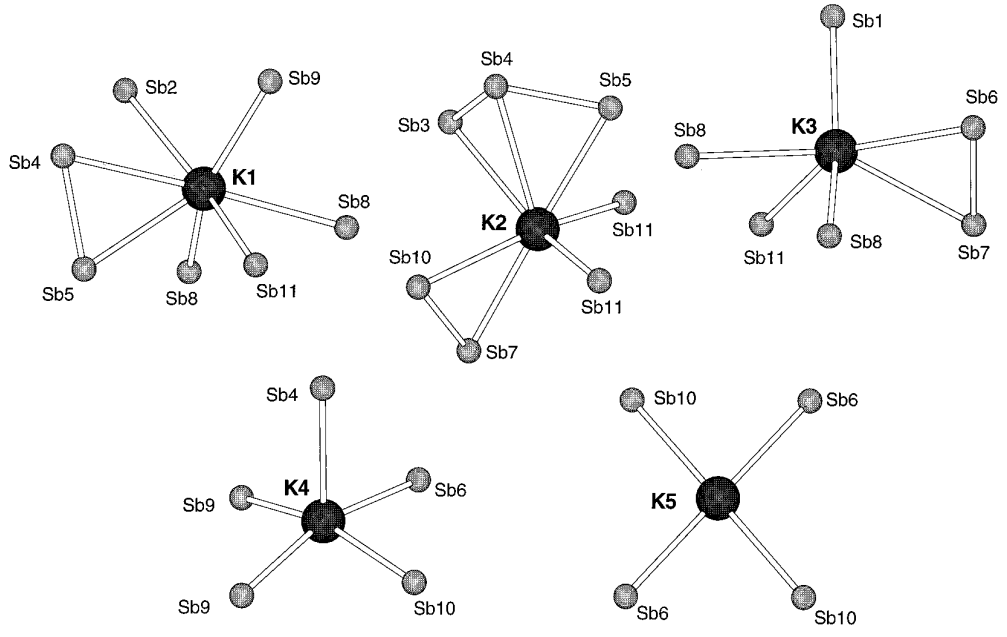

FIG. 5. Potassium coordination environments in compound **1**. See Table 3 for K^+ to layer Sb distances.

the synthesis and structures of the new quaternary Zintl phases $K_8In_8Ge_5As_{14}(As_3)$ and $K_5In_5Ge_5As_{10}(As_4)$ (13).

ACKNOWLEDGMENT

The work at North Carolina State University was supported by the U.S. Department of Energy, Office of Basic Sciences, Division of Materials Sciences, under Grant DE-FG05-86ER45259.

REFERENCES

1. (a) H. F. Klein, M. Gass, U. Koch, B. Eisenmann, and H. Schäfer, *Z. Naturforsch. B* **43,** 830 (1988); (b) G. Cordier, H. Schäfer, and M. Stelter, *Z. Naturforsch. B* **42,** 1268 (1987); (c) G. Cordier, H. Schäfer, and M. Stelter, *Z. Naturforsch. B* **41,** 1416 (1986); (d) G. Cordier, H. Ochmann, and H. Schäfer, *J. Less-Common Met.* **119,** 291 (1986); (e) G. Cordier, H. Schäfer, and M. Stelter, Z. *Naturforsch. B* **40,** 1100 (1985).
2. (a) W. Carrillo-Cabrera, N. Caroca-Canales, and H. G. von Schnering, *Z. Anorg. Allg. Chem.* **619,** 1717 (1993); (b) W. Carrillo-Cabrera, N. Caroca-Canales, K. Peters, and H. G. von Schnering, *Z. Anorg. Allg. Chem.* **619,** 1156 (1993).
3. (a) Q. Liu, R. Hoffmann, and J. D. Corbett, *J. Phys. Chem.* **98,** 9360 (1994); (b) Z. C. Dong and J. D. Corbett, *J. Am. Chem. Soc.* **116,** 3429 (1994); (c) Z. C. Dong and J. D. Corbett, *J. Am. Chem. Soc.* **115,** 11299 (1993); (d) A. K. Ganguli, A. M. Guloy, E. A.Leonescamilla, and J. D. Corbett, *Inorg. Chem.* **32,** 4349 (1993); (e) S. C. Sevov and J. D. Corbett, *Inorg. Chem.* **32,** 1612 (1993); (f) S. C. Sevov and J. D. Corbett, *J. Solid State Chem.* **103,** 114 (1993); (g) S. C. Sevov and J. D. Corbett, *Z. Anorg. Allg. Chem.* **619,** 128 (1993).
4. (a) G. Cordier and V. Muller, *Z. Naturforsch. B* **49,** 721 (1994); (b) W. Blase, G. Cordier, and M. Somer, *Z. Kristallogr.* **206,** 141 (1993); (c) W. Blase, G. Cordier, and M. Somer, *Z. Kristallogr.* **206,** 145 (1993); (d) G. Cordier and V. Muller, *Z. Kristallogr.* **205,** 133 (1993); (e) W. Blase, G. Cordier, and M. Somer, *Z. Kristallogr.* **203,** 146 (1993).
5. (a) M. Asbrand and B. Eisenmann, *Z. Kristallogr.* **205,** 323 (1993); (b) M. Asbrand and B. Eisenmann, *Z. Naturforsch. B* **48,** 452 (1993).
6. (a) R. G. Ling and C. Belin, *Z. Anorg. Allg. Chem.* **480,** 181 (1981); (b) M. Charbonnel and C. Belin, *New J. Chem.* **8,** 595 (1984); (c) R. G. Ling and C. Belin *J. Solid State Chem.* **45,** 290 (1982).
7. A. Ramos-Gallardo and A. Vegas, *Z. Kristallogr.* **210,** 1 (1995).
8. G. Cordier and H. Ochmann, *Z. Kristallogr.* **195,** 107 (1991).
9. G. Cordier and H. Ochmann, *Z. Kristallogr.* **197,** 291 (1991).
10. G. Cordier and H. Ochmann, *Z. Kristallogr.* **197,** 281 (1991).
11. W. Blase, G. Cordier, and M. Somer, *Z. Kristallogr.* **199,** 277 (1992).
12. S. Sportouch, M. Tillard-Charbonnel, and C. Belin, *Z. Kristallogr.* **209,** 541 (1994).
13. J. L. Shreeve-Keyer, Y.-S. Lee, S. Li, C. J. O'Connor, and R. C. Haushalter, submitted for publication.
14. A. F. Wells,'' Structural Inorganic Chemistry'' 5th ed. Oxford Univ. Press, Oxford, 1986.
15. J. H. C. Hogg and H. H. Sutherland, *Acta Crystallogr. Sect. B* **29,** 2483 (1973).
16. S. C. Sevov and J. D. Corbett, *Inorg. Chem.* **31,** 1895 (1992).
17. M.-H. Whangbo and R. Hoffmann, *J. Am. Chem. Soc.* **100,** 6093 (1978).